IEEE Access
Multidisciplinary ⋮ Rapid Review ⋮ Open Access Journal

Received 16 February 2023, accepted 12 April 2023, date of publication 18 April 2023, date of current version 4 May 2023.

Digital Object Identifier 10.1109/ACCESS.2023.3268072

RESEARCH ARTICLE

Occlusion-Aware Motion Planning for Autonomous Driving

DENGGUI WANG[1], WEIPING FU[1,2], JINCAO ZHOU[1], AND QINGYUAN SONG[1]
[1]School of Mechanical and Precision Instrument Engineering, Xi'an University of Technology, Xi'an 710048, China
[2]School of Engineering, Xi'an International University, Xi'an 710077, China

Corresponding author: Weiping Fu (weipingf@xaut.edu.cn)

This work was supported in part by the National Natural Science Foundation of China under Grant 52202501, and in part the Shaanxi Province Natural Science Basic Research Project through the Shaanxi Provincial Department of Science and Technology of China under Grant 2022JQ-546.

ABSTRACT Motion planning for autonomous vehicles remains a challenge in urban road environments with occlusions. In this study, we present a motion planning framework that prioritizes safety, comfort, and efficiency to enable autonomous vehicles to navigate safely through urban roads with occlusions. Our solution consists of three main components: local path planning, trajectory planning, and speed planning. First, based on the improved Artificial Potential Field to generate the local path, then the optimal trajectory is solved in the S-L coordinate with the local path as the reference line. Subsequently, the potential risk probability of the occluded area is incorporated into the incomplete information static game framework and implement speed planning based on the game results and the proposed vehicle "safe driving" to complete the collision avoidance between the autonomous vehicle and visible or obscured dynamic traffic participants. In high pedestrian traffic scenarios, simulation verification shows that the proposed model enhances autonomous vehicle comfort levels by about 32%∼48% compared to the baseline method utilizing automatic emergency brake system (AEB). We also conducted simulation verification of the proposed model in overtaking and left-turning traffic scenarios, comparing it with other models. The results demonstrate that our proposed model ensures safe autonomous driving in traffic scenario with occlusions while maintaining comfort and efficiency.

INDEX TERMS Autonomous vehicles, collision avoidance, motion planning, path planning, speed planning, visual occlusion.

I. INTRODUCTION

The primary goal of motion planning for autonomous driving is to determine a secure trajectory for autonomous vehicles (AVs). However, in the context of urban road environments, numerous sources of uncertainty pose significant challenges to achieving this objective. Although AVs are equipped with various sensors. the urban road environment is not only populated by a variety of motor vehicles, but is also usually surrounded by obstacles such as parked vehicles, buildings, construction fences, green belts and bridges, etc. Moving vehicles and stationary obstacles cause on-board sensor visual occlusion, which prevents the AV from fully observing the surrounding environment, as shown in Fig. 1. However, developing a motion planner that covers all possible situation is a tedious process and even impractical, especially in autonomous driving scenarios. Most AVs perform motion planning based on observed environmental information. For safe, efficient and comfortable driving, it is necessary to properly incorporate unobservable risks, such as those caused by occlusions, into motion planning.

Most existing solutions incorporate static occlusions into motion planning, which has achieved remarkable results. However, this method cannot adapt well to a situation where the sensor is dynamically occluded by moving obstacles [1]. In this paper, the results of our previously proposed method in [2] for potential risk assessment of occluded areas are applied to the autonomous motion planning task. A novel AV

The associate editor coordinating the review of this manuscript and approving it for publication was P. Venkata Krishna.

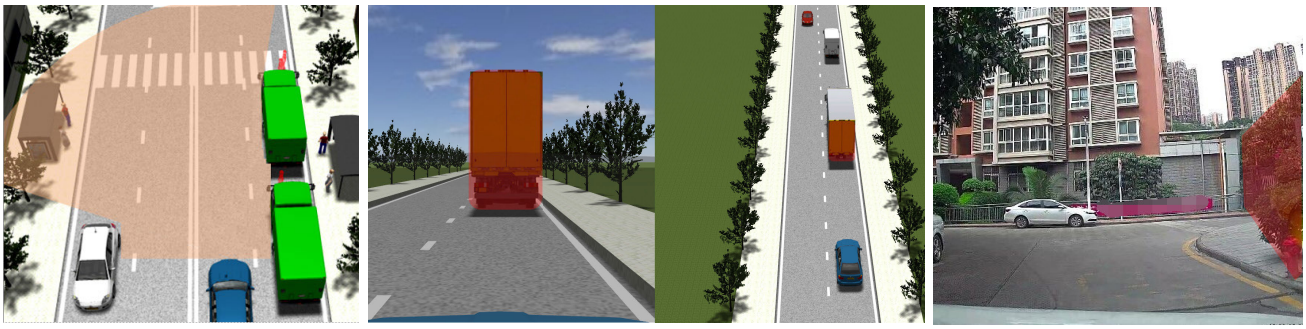

(a) (b) (c)

FIGURE 1. Common occlusion scenarios that create challenges and safety risks for autonomous vehicles. (a) The blue car is an AV, and pedestrians crossing the road are occluded by parked vehicles; (b) AV's line of sight was obstructed by a large vehicle prior to overtaking; (c) The autonomous vehicle proceeded into an intersection with obstructed right-side visibility.

motion planning method considering driving scenarios with visual occlusion is proposed, which enables the AV to react safely if other traffic participant unexpectedly emerges from an occluded area while ensuring a comfort and efficiency. The simulation experiment shows that such risk-aware policy can be more reliable and safer at challenging situations without being overcautious comparing to some previous works that only consider the rule-based policy.

The main contributions of this paper are as follows:

- A motion planner is presented that is capable of actively adjusting the heading and speed of autonomous vehicles based on their surroundings, enabling safe driving in various scenarios including visual occlusion.
- Local path planning based on the improved Artificial Potential Field and trajectory planning in S-L coordinates are adopted to overcome the uncertainty of various physical obstacles in motion planning.
- For the first time, risk probabilities have been incorporated into a virtual game strategy with incomplete information to complete AV speed planning in the presence of occluded traffic obstacles.

The remainder of the paper is structured as follows: In section II, we discuss existing work on occlusion-aware motion planning of autonomous driving. In section III, the proposed AV motion planning method is described in detail in terms of three modules: local path planning, trajectory planning and speed planning. In Section IV, the validity of proposed method is verified by simulations and experiments in different representative driving scenarios and demonstrates the advantages of the proposed method. Section V draws conclusions and points out future research directions.

II. RELATED WORD

As the application area of AVs continues to broaden, sensor occlusion becomes inevitable and the number of studies on occlusion-aware motion planning has been increasing in recent years. Some earlier studies considered only occlusions caused by static obstacles around the AV [3], [4], [5], [6]. It is convenient to limit the study to static occlusions because the evolution of the field of view scenario only depends on the location of the AV, which can be estimated if high-resolution map is available. Recent works have tackled the dynamic occlusion, such as [7], [8], [9], and [10], although each of them considered only a specific traffic scenario.

The occlusion-aware motion planning solution must generate state trajectories that indicate the potential response of the AV if an occluded agent emerges from an occluded area [8]. Safety maneuvers that an AV should be able to perform usually include braking before a certain interaction area. Some studies proposed utilizing external information provided by the road infrastructure to ensure safe navigation of AVs [11], [12], In [11] additional external sensing data transmitted via low-latency mobile networks used in parallel with the onboard perception module to plan safe and comfortable motion of passengers. While the use of additional information from external sources can improve the perception of surrounding occluded areas by AVs, high-quality networks that reliably transmit the necessary information in real time are usually required, in addition, these infrastructures cannot guarantee adequate coverage of all regions, so widespread adoption of approaches that rely on information from external sources can be slow.

A common strategy for mitigating the risk of collision with occluded agents is to assume a virtual agent is always present in the occluded area and move away from the visible region boundary at a constant velocity [13], [14], [15], [16]. Based on such an assumption, the collision time TTC of the AV with the virtual agent can be calculated, and by regulating the speed of the AV collisions with these virtual agents can be avoided. The advantage of this approach is that it is relatively reliable, and the resulting behavior is easy to interpret. However, it also has limitations, first, the TTC model assumes a constant speed, which ignores almost all information about the agent's intention. Second, in many cases, agents using TTC are overly cautious, causing unnecessary delays.

Reachability analysis is used to describe the set of states that any potentially occluded vehicle can reach and to plan safety trajectories accordingly [3], [4], [15], [17], [18]. In general, a set of states represents all possible configurations that traffic participants may reach. Yu et al. [17], [18] applied a sampling method to represent potentially occluded agent states as particles, through bidirectional reachability

analysis, the distribution of dangerous "phantom" objects was determined. Although the safety of this method was demonstrated, reachability analysis can lead to conservative driving behavior in some exceptional situations with limited visibility. In such cases, it is necessary for the AV to enter the conflict zone cautiously to gather more information and prevent deadlock.

Several researchers have proposed data-driven approaches to learn the basic features of such safety behaviors [19]. However, data-driven deep learning methods based on data must rely on large amounts of data samples for training, and the learned models do not adapt well to unfamiliar environments.

Apart from the more common techniques mentioned above, Partially Observable Markov Decision Processes (POMDP) have been widely used in occlusion-aware motion planning [20], [21], [22], [23], [24], [25]. For example, the collision avoidance of self-driving cars performs very well under state uncertainty thanks to the POMDP algorithm in [20] and [21]. Although POMDP solutions can generate low-conservative strategies, it does not guarantee or focus on safety and this approach usually suffer from high computational burden, requires a reduced state space to make the algorithm computationally tractable. In [26], [27], and [28], driving strategies at occluded urban intersections are obtained using Reinforcement Learning (RL). Kamran et al. [29] used a risk-aware deep Q-network (DQN) to deal with occluded intersections. Instead of considering only collisions, the risk assessment is incorporated into the reward function. If an intersection is blocked, the vehicle is assumed to have the maximum allowed speed. In [19] and [30], effective driving behaviors are learned directly from expert driving data of drivers at low-visibility intersections by feature extraction. Similarly, in [31], expert driving data is used to determine the parameters of the risk potential function for uncontrolled intersections, which is ultimately used to determine the safe speed of the AV.

Some studies have minimized occlusion and improved visibility by actively adjusting the lateral position of self-vehicles to increase the chance of detection of occluded traffic participants earlier [7], [32], [33]. While these methods have been shown to produce effective driving behavior when encountering occlusions, their main limitation is that their ability to be applied in scenarios other than those for which they were specifically designed is not guaranteed.

Inspired by works [34] and [35], we incorporate the Probability distribution of agent emergence from obscured regions predicted from contextual information which obtained in previous work [2] into the incomplete information virtual game to regulate the speed of the autonomous vehicle on motion planning.

III. MOTION PLANNING

The motion planning model proposed in this paper is decomposed into three parts: local path planning, trajectory planning, and speed planning. Local path planning completes the static environment's path solution, while trajectory planning completes the dynamic trajectory planning and solves the optimal trajectory. Speed planning addresses collision problems between AVs and various moving obstacles, including obscured moving objects.

A. VEHICLE MODEL

Suppose that in the two-dimensional space, we have an AV e and other interactive agents $o = \{o_1, o_2, \cdots, o_n\}$, in the global inertial coordinate system, the AV states can be described as:

$$S_e = [x, y, \varphi, v, \kappa, \alpha] \tag{1}$$

where (x, y) denotes the position, φ is the heading angle, κ denotes the curvature, i.e., the rate of change of the heading angle, v and α denote the velocity and acceleration of the AV, respectively. The vehicle kinematics model of the AV is

$$\begin{aligned} \dot{x} &= v\cos\varphi \\ \dot{y} &= v\sin\varphi \\ \dot{\varphi} &= v\kappa \\ \dot{v} &= \alpha \\ \kappa, \alpha &= \text{input} \end{aligned} \tag{2}$$

In this paper, the control inputs consist of acceleration and curvature. AV state change is driven by the change of speed and heading angle by the control inputs $c = [\kappa, \alpha]^T$, where κ is the output of the trajectory planner and α is the output of the speed planner.

B. LOCAL PATH PLANNING

Safe and efficient local path planning is crucial for ensuring the safe and smooth operation of self-driving cars. However, due to the highly dynamic nature of road environments, it is imperative to quickly and accurately identify unpredictable obstacles and make necessary adjustments to the local path.

The Artificial Potential Field (APF) is mainly applied in the field of robot obstacle avoidance [36], and a modern car can be regarded as a high-speed robot, so this method can also be applied in the field of obstacle avoidance path planning for cars. However, the APF also suffers from the problem of excessive target gravitational force, the problem of target unreachability and the tendency to fall into local minima, which can lead to path planning failure in complex environments. We propose a path planning method based on improved APF, aiming to study the influence range of the gravitational field function and repulsive field function in the process of obstacle avoidance by using a distance threshold and repulsion adjustment factor.

For the problem of excessive gravitational force at the target position, the improved gravitational field function $U_{att}(p)$ is:

$$U_{att}(p) = \begin{cases} \frac{1}{2}\eta_{att}\rho_{eg}^2, & 0 < \rho_{eg} \le d_g \\ d_g\eta_{att}\rho_{eg}, & 0 < \rho_{eg} \le d_g \end{cases} \tag{3}$$

where η_{att} is the gravitational gain coefficient, ρ_{eg} is a vector that denotes the Euclidean distance between the current position of the AV and the target position, and d_g is a set distance threshold for the influence of the target point on the AV. The corresponding gravitational force, $F_{att}(p)$, is the negative gradient of the gravitational field:

$$F_{att}(p) = -\nabla U_{att}(p) = \begin{cases} -\eta_{att}\rho_{eg}, & 0 < \rho_{eg} \le d_g \\ -d_g\eta_{att}\dfrac{\rho_{eg}}{\| \rho_{eg} \|}, & 0 < \rho_{eg} \le d_g \end{cases} \tag{4}$$

Formula (4) indicates that the gravitational force is proportional to ρ_{eg} when ρ_{eg} is less than d_g; otherwise, the gravitational force is constant.

To address the problems of target unreachability and local minima, by improving the repulsive force potential field function of the obstacles to be solved, a common method is to add a modulation factor ρ_{eg}^n to the repulsive field model so that the repulsive and gravitational forces are reduced to zero simultaneously only when the car reaches the target point. The improved repulsive field function, $U_{req}(p)$, is:

$$U_{req}(p) = \begin{cases} \dfrac{1}{2}\eta_{req}\left(\dfrac{1}{\rho_{eo}} - \dfrac{1}{d_o}\right)^2 \rho_{\mathrm{eg}}^n, & 0 \le \rho_{eo} \le d_o \\ 0, & \rho_{eo} > d_o \end{cases} \tag{5}$$

where η_{req} is the repulsion gain coefficient, ρ_{eo} is a vector that denotes the Euclidean distance between the current position of the AV and the obstacle, and d_o represents the maximum range of influence of the obstacle on the AV, it should be noted that d_o takes different values depending on whether the obstacle is in the same lane as the autonomous vehicle. In this paper, we set $n = 2$. The corresponding repulsive force, F_{req}, is the negative gradient of the repulsive field:

$$F_{req}(p) = \begin{cases} \eta_{req}\left(\dfrac{1}{\rho_{eo}} - \dfrac{1}{d_o}\right)\dfrac{\rho_{\mathrm{eg}}^n}{\rho_{\mathrm{eo}}^2} + \dfrac{n}{2}\eta_{req}\left(\dfrac{1}{\rho_{eo}} - \dfrac{1}{d_o}\right)^2 \rho_{\mathrm{eg}}^{n-1}, & 0 \le \rho_{eo} \le d_o \\ 0, & \rho_{eo} > d_o \end{cases} \tag{6}$$

The area of AV travel is restricted by establishing a road boundary repulsive potential field:

$$U_{req,edge}(y) = \begin{cases} \dfrac{1}{2}\eta_{edge}\left(\dfrac{1}{\rho_y} - \dfrac{1}{d_y}\right)^2, & 0 \le \rho_y \le d_y \\ 0, & \rho_y > d_y \end{cases} \tag{7}$$

The corresponding repulsive force is:

$$F_{req,edge}(y) = \begin{cases} \eta_{edge}\left(\dfrac{1}{\rho_y} - \dfrac{1}{d_y}\right)\dfrac{1}{\rho_y^2}, & 0 \le \rho_y \le d_y \\ 0, & \rho_y > d_y \end{cases} \tag{8}$$

where η_{edge} is the repulsion gain coefficient. It should be noted that η_{edge} should be taken separately for different repulsive potential fields at the road boundary and at the solid and dashed lines of the lane boundary. ρ_y is the value of the lateral distance between the AV and the center point of the repulsive potential field, and d_Y denotes the maximum range of influence of the repulsive potential field acting on the AV.

The combined potential field in the entire driving area is the sum of the gravitational and repulsive potential fields, and the combined force on the AV is the sum of the gravitational and repulsive forces.

$$\begin{cases} U_{sum}(p) = U_{att}(p) + \sum U_{req}(p) + \sum U_{req,edge}(y) \\ F_{sum}(p) = F_{att}(p) + \sum F_{req}(p) + \sum F_{req,edge}(y) \end{cases} \tag{9}$$

The path planning results for the AV in moving to the target position p_g, visualizing the combined potential field and describing the forces on the AV at position p_e as show in Fig. 2. The results show that under the joint action of road gravitational potential field, obstacle repulsion potential field and road repulsion potential field, AV can complete local path planning.

C. TRAJECTORY PLANNING

Local path planning is carried out without considering moving obstacles and vehicle dynamics constraints, and the planned path does not guarantee sufficient safety and comfort of the vehicle. Trajectory planning is to take the above planned path as the reference line and plan the optimal trajectory of the vehicle considering the actual moving obstacles and vehicle dynamics constraints.

1) ROAD COORDINATE

Due to the diversity of traffic road alignment, it is very troublesome to make the road discretization using only inertial X-Y coordinate. As in the literature [37], to overcome this problem, we adopt $S-L$ curvilinear coordinate to accomplish the dynamic trajectory planning. The trajectory planning algorithm relies heavily on the definition of reference line, a sampling function $r(s)$ can be used to define the reference lines in the road.

$$r(s) = [x_r(s), y_r(s), \varphi_r(s), \kappa_r(s)] \tag{10}$$

where, s represents the arc length along the reference line, $(x_r(s), y_r(s))$ represents the position of the sample point in $S-L$ curvilinear coordinate, $\varphi_r(s), \kappa_r(s)$ represent the tangent direction and curvature of the sample point, respectively. As shown in Fig. 3, we can define a vehicle state point $p(s, l)$ away from the reference line:

$p(s, l) = [x_p(s, l), y_p(s, l), \varphi_p(s, l), \kappa_p(s, l)]$, l represents the lateral offset relative to the reference line, also called the lateral displacement. The relationship of $p(s, l)$ with coordinate system and the reference line sampling

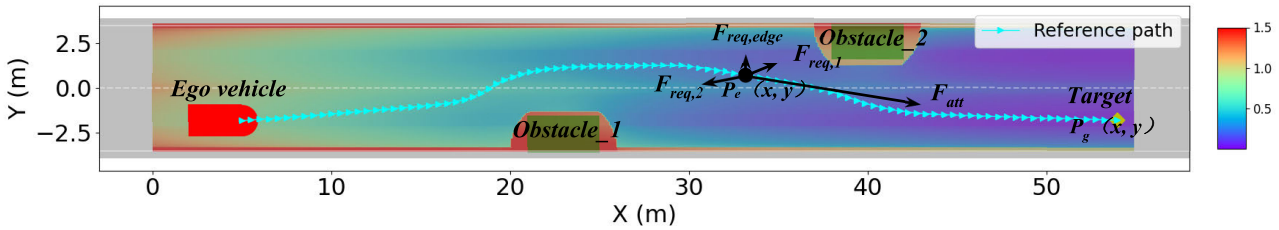

FIGURE 2. Artificial Potential Field-based local path planning.

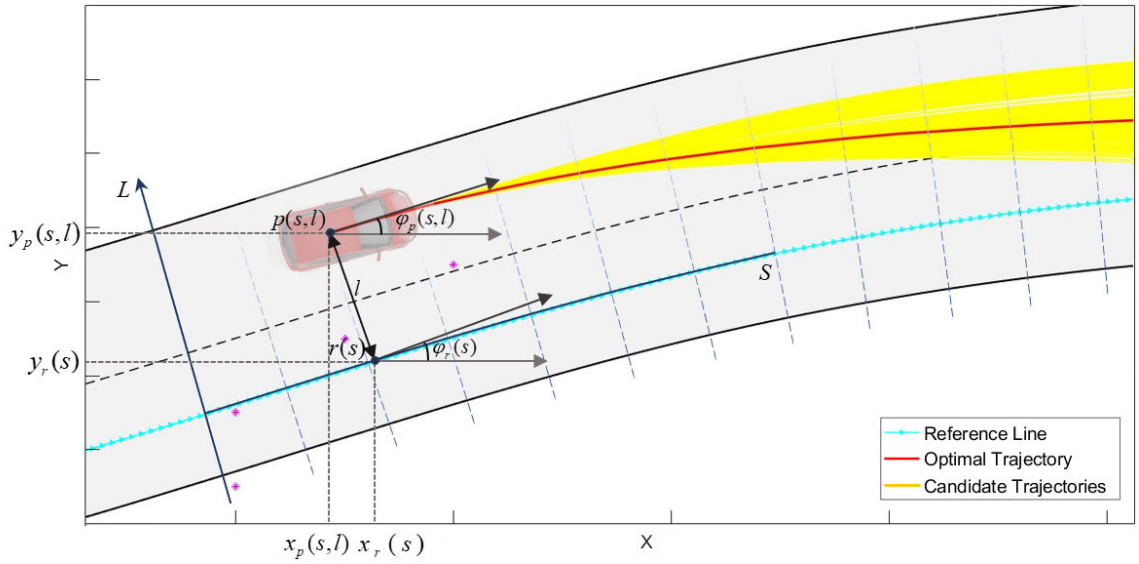

FIGURE 3. Trajectory planning in S-L coordinate.

function satisfies:

$$\begin{aligned} x_p(s,l) &= x_r(s) + l\cos(\varphi_r(s) + \pi/2) \\ y_p(s,l) &= y_r(s) + l\sin(\varphi_r(s) + \pi/2) \\ \varphi_p(s,l) &= \varphi_r(s) + \arctan(dl/ds) \\ \kappa_p(s,l) &= (\kappa_r(s)^{-1} - l)^{-1} \end{aligned} \tag{11}$$

Trajectory produced by our planner express the motion of the AV as a function of curvature κ with respect to the arc length s along the reference line, in which case we express the vehicle model as:

$$\begin{aligned} dx/ds &= \cos(\varphi(s)) \\ dy/ds &= \sin(\varphi(s)) \\ d\varphi/ds &= \kappa(s) \end{aligned} \tag{12}$$

The Formula (12) shows that the AV position state is determined by the curvature. Thus, for the trajectory planner, local trajectories can be carried out by determining the curvature.

2) CANDIDATE TRAJECTORY GENERATION

A trajectory can be viewed as a sequence of vehicle states, and it is generated by connecting sampled endpoints using various types of curvature polynomials. The connection method employed in our planner is identical to that described in [37]. However, quintic curvature polynomials are utilized instead of cubic ones to ensure the continuity of the rate of change in curvature at the beginning point of each planning cycle. The curvature can be defined as a quintic polynomial function with respect to arc length.

$$\kappa(s) = k_0 + k_1 s + k_2 s^2 + k_3 s^3 + k_4 s^4 + k_5 s^5 \tag{13}$$

where a set of parameters can determine a trajectory, so the problem becomes to find the parameters satisfying the endpoint constraints, we use a gradient descent algorithm to solve this problem.

When the vehicle drives on the road, the initial state $p_{init} = (x_I, y_I, \varphi_I, \kappa_I)$ and the desired state $p_{goal} = (x_G, y_G, \varphi_G, \kappa_G)$ are given. To reduce the magnitude error among the parameters, it is required the parameters to be solved for should be of a similar scale, we introduce new parameters $\mathbf{p} = [p_0, p_1, p_2, p_3, p_4, p_5, s_G]$ to reformulate the function (13) as:

$$\kappa(s) = a(\mathbf{p}) + b(\mathbf{p})s + c(\mathbf{p})s^2 + d(\mathbf{p})s^3 + e(\mathbf{p})s^4 + f(\mathbf{p})s^5 \tag{14}$$

where

$$\kappa(0) = p_0 = \kappa_I, \quad d\kappa(0) = p_1 = d\kappa_I, \; d^2\kappa(0) = p_2 = d^2\kappa_I$$
$$\kappa(s_G/3) = p_3, \quad \kappa(2s_G/3) = p_4, \; \kappa(s_G) = p_5 = \kappa_G$$

There are seven parameters in the function (14), we note that $p_0 = \kappa_I, p_1 = d\kappa_I, p_2 = d^2\kappa_I$ and $p_5 = \kappa_G$. This leaves just three unknowns $[p_3, p_4, s_G]$, using the gradient descent algorithm, we can quickly find the parameters of a quintic curvature polynomial that is very close to the initial state limit.

3) CANDIDATE TRAJECTORY FILTERING

There are safety constraints on the motion and dynamics of the vehicle, to reduce the burden of the system and speed up the calculation, the trajectories that cannot satisfy the limit conditions can be filtered by trajectory filtering before calculating the optimal trajectory. The main task of filtering includes curvature filtering and collision filtering.

For curvature filtering, the retained trajectories need to satisfy

$$\kappa_j[i] \le \kappa_{\max}, \quad 0 \le j \le N \tag{15}$$

where $\kappa_j[i]$ is the curvature of the trajectory i at trajectory point j after discretization in the S direction, $\kappa_{\max}$ is the maximum curvature set for comfort, N is the maximum number of trajectory points after discretization.

For collision filtering, the retained trajectory needs to satisfy that the distance between any point j on trajectory i and the obstacle (x_{ob}, y_{ob}) is greater than the safety distance d_{safe}.

$$(x_i - x_{ob})^2 + (y_i - y_{ob})^2 \ge d_{safe}^2 \tag{16}$$

The retained trajectories after filtering are the candidate trajectory of the AV, as shown in the yellow profiles in Fig. 3.

4) TRAJECTORY OPTIMIZATION

The goal of trajectory optimization is to find the smoothest trajectory curve with the lowest cost function among all the trajectories retained after trajectory filtering, as shown in the red profile in Fig. 3. Consider the trajectory curve ι, which is connected by trajectory points $(n_0, n_1, \cdots, n_m)$, and its cost function can be written as

$$Cost(\iota) = \Omega(\iota) + \Phi(\iota) \tag{17}$$

where $\Omega(\iota)$ represents the cost accumulated by traveling along this trajectory curve, and $\Phi(\iota)$ represents the cost introduced by this trajectory ending at this end point.

We consider the following factors to design the $\Omega(\iota)$ function.

- The optimal trajectory should closely follow the reference line, and any deviation from it will result in an increase in the cost of the trajectory.
- The optimal trajectory is capable of real-time obstacle avoidance and maintaining a safe distance from obstacles.
- The optimal trajectory should minimize large changes in curvature (including its derivatives) to ensure passenger comfort.

For the calculation of the $\Phi(\iota)$, since we solve the speed planning as a separate problem, the cost function of $\Phi(\iota)$ can consider only the longitudinal displacement part of the trajectory.

$$\Phi(\iota) = -\omega_s s_G(\iota) + h_d(s_G(\iota)),$$
$$h_d(s) = \begin{cases} -\omega_d & \text{if } s \ge s_{threshold} \\ 0 & \text{otherwise} \end{cases} \tag{18}$$

where $-\omega_s s_G(\iota)$ is a linear cost that represents the overall trajectory biased towards trajectories with longer longitudinal displacements s, the negative sign represents a reduction in cost, while $h_d(s)$ is a nonlinear cost that is triggered only when the overall longitudinal displacement s exceeds a certain threshold.

D. SPEED PLANNING

After the optimal trajectory is selected, speed planning designs what speed is used to travel this trajectory. The variation of speed is controlled by the control input variable α. For the visual occlusion, the planned speed in various situations (whether an agent unexpectedly emerge from the occluded area or not) should ensure both the safety and comfort of autonomous vehicle driving, also consider the driving efficiency. In this subsection, we first describe in detail the proposed "virtual game" model between the AV and occluded agents, and then give an acceleration setting scheme.

1) THE GAME OF AV AND OCCLUDED AGENTS

For the potential collision risk in occluded areas, deceleration with worst-case assumptions leads to overly conservative AV behavior [38], which is unacceptable to consumers. To address this issue, some systems rely on automatic emergency braking (AEB) to prevent collisions [23], [39]. However, unnecessarily frequent activation of AEB can reduce AV comfort in potentially risky and intermittently occluded scenarios.

To overcome these problems, the main idea of our approach is, first, to predict the potential risk probability λ_c generated by the occluded area to the AV adopting the method in our previous work [2]; secondly, to compare λ_c with the risk probability threshold λ_{th} proposed below, the AV selects different operations according to different situations:

When $\lambda_c \ge \lambda_{th}$, AV with the safety and comfort of operation as the main goal, uses a relatively low deceleration reduce speed when approaching the interaction area to prevent a collision with a suddenly appearing traffic participant.

When $\lambda_c < \lambda_{th}$, the AV with safety and efficiency as the main goal, moves forward at the maximum safe speed when approaching the interaction area and activates emergency braking only when an object unexpectedly exits the occluded area, since this phenomenon is, after all, a rare occurrence.

a: POTENTIAL RISK PROBABILITY

The potential risk probability λ_c refers to the probability that a traffic participant who poses a collision risk to an AV will emerge from the occluded area. We used the Bayesian network-based model in our previous work [2] to predict the potential risk probabilities. The value of λ_c is be predicted and inferred by AVs by observing the states of environmental impact factors, such as divider, crosswalk, traffic flow, number of lanes, obstacle speed, etc. Since the potential risk probability assessment is more complex and this paper only uses the assessment results, so it is not described in detail, for details, please see reference [2].

b: RISK PROBABILITY THRESHOLD

A risk can be ignored if the potential risk probability value is less than the risk probability threshold. In this paper, a static game method is used for the analysis and calculation of λ_{th}. Some studies describe the multiagent interaction problem (car-to-car and car-to-person) without occlusions as a complete information game problem [40] and [41]. This paper studies the vehicle interaction problem on urban roads with visual occlusion. If a complete information game is used, the structural characteristics of the game are uncertain, and the payoff function in the game process is not common knowledge. Therefore, complete information cannot be used for game analysis. Based on the Harsanyi transform [42], we developed a model of a static "virtual game" with incomplete information to analyze the above problem.

It is assumed that the uncertainty agent *o_agent* in the occluded area is composed of two classes of deterministic agents, namely, the "present agent (*p_agent*)" and the "absent agent (*a_agent*)". The *p_agent* refers to an agent that "exists" in the occluded area, which will pose a threat to the AV. Considering the perceptual decision-making capabilities of such agents, this threat is probabilistic. The *a_agent* refers to an agent that "may not exist" in the occluded area, which does not pose a threat to the AV. In addition, it is assumed that all agents have two personality characteristics "*p* (proactive)" and "*y* (yield)" regarding the right of way. When there is interaction between agents, "*p*" indicates that the agent tends to seize the right of way, while "*y*" indicates that the agent tends to give up the right of way. Since *p_agent* and *a_agent* are descriptions of virtual agents in the occluded area, these two types of agents are regarded as "players" who play a game with the AV i.e. *e_agent*, which is called a "virtual game". Agents with different personality characteristics lead to different situations when they play interactive games. Fig. 4 shows the payoff matrix of *e_agent* and *o_agent* in the "virtual game".

Fig. 4 is analyzed from a safety point of view. First, the analysis of *e_agent* is as follows: (i) If *o_agent* is "*p_agent*": when *p_agent* selects the "*p*" feature, the payoff $(u_{yp}^{p,e}, u_{yp}^{p,o})$ of both parties is optimal. If the feature of *p_agent* is "*y*", when *e_agent* selects the"*p*" feature, the payoff $(u_{py}^{p,e}, u_{py}^{p,o})$ of both parties is optimal. At this point, there are two pure

		o_agent			
		p_agent		*a_agent*	
		p	*y*	*p*	*y*
e_agent	*p*	$u_{pp}^{p,e}, u_{pp}^{p,o}$	$u_{py}^{p,e}, u_{py}^{p,o}$	$u_{pp}^{a,e}, u_{pp}^{a,o}$	$u_{py}^{a,e}, u_{py}^{a,o}$
	y	$u_{yp}^{p,e}, u_{yp}^{p,o}$	$u_{yy}^{p,e}, u_{yy}^{p,o}$	$u_{yp}^{a,e}, u_{yp}^{a,o}$	$u_{yy}^{a,e}, u_{yy}^{a,o}$

FIGURE 4. Payoff matrix for games with incomplete information.

strategic Nash equilibria in the game, namely $(u_{yp}^{p,e}, u_{yp}^{p,o})$ and $(u_{py}^{p,e}, u_{py}^{p,o})$. (ii) If *o_agent* is "*a_agent*": Since the main performance characteristic of *a_agent* is that it will not pose a threat to the AV. Whether the *a_agent* feature is "*p*" or "*y*", for *e_agent*, the self-revenue value is greater when selected the "*p*" feature than the self-revenue when selected the "*p*" feature. In this case, *a_agent* is safer when the feature of *a_agent* is "*y*", the game has a unique Nash equilibrium, namely $(u_{yp}^{p,e}, u_{yp}^{p,o})$. By the above analysis, for *e_agent*, the type of *o_agent* is not known when playing with *o_agent*. For this incomplete information game problem, the related methods of the complete information game cannot be used to solve it.

The Harsanyi transformation provides a solution for the problem of incomplete information in games. A virtual "player", "*nature*", is introduced into the original game to construct a three-player game with players *e_agent*, *o_agent* and *nature*, as shown in Fig. 5. First, *nature* selects the feature of *o_agent*, then, *e_agent* and *o_agent* play a game. The selection result of *nature*, *e_agent* is indeterminate, but *o_agent* is certain. In the newly constructed three-player game, the payoff of *nature* does not need to be considered, and the payoffs of *e_agent* and *o_agent* are determined by Fig. 4.

Obviously, the H-transform turns an incomplete information game problem into a complete but imperfect information game problem. However, the complete information game processing method cannot be directly applied to the solution. In Fig. 5, the "virtual" participant "*nature*" has no payoff or the payoff is not considered. That is, the feature of *o_agent* is random. It should be noted that the participant *nature* randomly selects the feature of *o_agent*. Therefore, *e_agent* must provide an action inference about *nature* when deciding its choice, which can be represented by a probability distribution. λ represents the probability that *e_agent* thinks that *nature* will select *o_agent* as *p_agent*, i.e., there is a potential risk probability for the occluded area.

$u_e(p)$ and $u_e(y)$ represent the expected benefits that *e_agent* thinks it can obtain when it chooses actions "*p*" and "*y*", respectively. χ represents the probability that *o_agent* selects feature "*p*". Since

$$\begin{bmatrix} u_e(p) \\ u_e(y) \end{bmatrix} = \lambda \begin{bmatrix} u_{pp}^{p,e}, u_{py}^{p,e} \\ u_{yp}^{p,e}, u_{yy}^{p,e} \end{bmatrix} \begin{bmatrix} \chi \\ 1-\chi \end{bmatrix} + (1-\lambda) \begin{bmatrix} u_{pp}^{a,e}, u_{py}^{a,e} \\ u_{yp}^{a,e}, u_{yy}^{a,e} \end{bmatrix} \begin{bmatrix} \chi \\ 1-\chi \end{bmatrix}$$

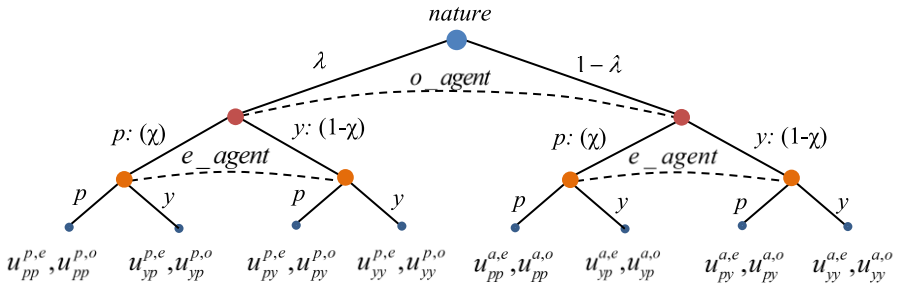

FIGURE 5. Game tree after introducing virtual player "nature."

$$0 \le \lambda \le 1,\ 0 \le \chi \le 1 \tag{19}$$

for *e_agent*, when $u_e(p) > u_e(y)$, its optimal choice is "p" that is, take the right of way and move forward. When $u_e(p) \le u_e(y)$, its optimal choice is "y", that is, to yield the right of way. Because $0 \le \chi \le 1$, given the value of χ, the threshold λ_{th} can be obtained according to Formula (20):

$$\lambda_{th} = \{\lambda | \exists \chi \in R, \quad 0 \le \chi \le 1, \quad \arg \max_{0 \le \lambda \in R \le 1} (u_e(p) - u_e(y) > 0) \tag{20}$$

Based on references [43] and [44], when potential traffic participants cross the road illegally, $\chi = 0.15$; otherwise, $\chi = 1$. Using the potential risk assessment values from our previous work [2], i.e., $\lambda = \lambda_c$, when $\lambda < \lambda_{th}$, the optimal choice of the AV (*e_agent*) is "p", and it will accelerate or maintain a constant speed. When $\lambda \ge \lambda_{th}$, the optimal choice of the AV is "y", and it will perform a deceleration operation.

2) ACCELERATION SETTING

When there is no risk, the AV accelerates to achieve the desired speed or run at a constant speed. When the AV encounters an obstacle or a potential risk of visual occlusion, deceleration can eliminate or reduce the risk of a collision. According to Formula (2), the speed behavior (acceleration, constant speed, or deceleration) of the AV depends on control input α.

a: DECELERATION

When the AV decelerates, the speed planning function is:

$$\alpha = \frac{1 - e^{-(v_e - v_{obs})^2/2\sigma_{obs,v}^2}}{1 + e^{-(v_e - v_{obs})^2/2\sigma_{obs,v}^2}} \cdot \mu \cdot \alpha_{\min} \quad s.t. \begin{cases} \mu = 1 & \lambda_c < \lambda_{th} \\ 0 < \mu < 1 & \lambda_c \ge \lambda_{th} \end{cases} \tag{21}$$

where v_{obs} is the speed of the obstacle or potential area of danger in the moving direction of the AV; $a_{min} < 0$ is the absolute maximum deceleration of the AV; $\sigma_{obs,y}$ is the action range of the obstacle on the AV. The expression $(1-e^{-(v_e-v_{obs})^2/2\sigma_{obs,y}^2})/(1+e^{-(v_e-v_{obs})^2/2\sigma_{obs,y}^2})$ with the Gaussian distribution model represents that the greater the difference between v_e and v_{obs} is, the greater the AV speed change, and the farther away the obstacle or potential field of danger is, the smaller the impact on the AV. μ is a coefficient that balances the comfort and efficiency of the AV by adjusting the acceleration according to the potential risk value when the AV speed changes.

b: ACCELERATION

Compared with deceleration motion, AV acceleration motion considers fewer elements. The purpose of acceleration is to achieve the desired speed when obstacles or potential occlusion risks have no effect on the AV. Similar to deceleration motion, AV acceleration motion or car-following is established as follows:

$$\alpha = \frac{1 - e^{-(v_e - v_{des})^2/2\sigma_{des,v}^2}}{1 + e^{-(v_e - v_{des})^2/2\sigma_{des,v}^2}} \alpha_{des} \tag{22}$$

where v_{des} is the expected speed of the AV, with a standard deviation of $\sigma_{des} > 0$. $(1 - e^{-(v_e - v_{\text{des}})^2/2\sigma_{des,v}^2})/(1 + e^{-(v_e - v_{des})^2/2\sigma_{des,v}^2})$ with a Gaussian distribution model represents the effect of $v_e - v_{des}$ on changes in v_e. The larger $v_e - v_{des}$ is, the larger the AV speed change. $\alpha_{des} > 0$ is the desired acceleration set considering efficiency and comfort when the AV accelerating.

IV. SIMULATION VALIDATION

Finally, the validity of proposed method is verified by simulations. Three typical driving scenarios involving occlusion are designed to describe the implementation details of the method. The proposed method is applied in autonomous driving motion planning in urban road scenes with visual occlusion by comparison with previous work [18], [39], and the benefits are analyzed. The relevant parameters in the experiment are listed in Table 1.

According to Formulas (19) and (20):

$$\lambda_{th} = \begin{cases} 0.04, & \chi = 1 \\ 0.21, & \chi = 0.15 \end{cases}$$

A. SAFE DRIVING

We first propose a definition for "safe driving" of AV, we suppose that the ordinary differential of each agent state

TABLE 1. Part parameters for simulation experiment.

Parameter	Value
Data sampling interval: Δt	*0.1 s*
Pedestrian speed: v_p	*1.5 m/s*
Virtual vehicle speed: v_o	$v_{limt} \pm 10\%$
Maximum curvature: $\kappa_{\max}$	1 *1/m*
Safe distance : $d_{sef,v-p}$	*Vehicle-pedestrian: 1.4 m*
Safe distance : $d_{sef,v-v}$	*Vehicle- vehicle: 3 m*
Acceleration: a_{des}	*3 m/s²*
Deceleration: $a_{\min}$	*-7 m/s²*
Coefficient: μ	$\lambda_c \geq \lambda_{th}$: *0.5* $\lambda_c < \lambda_{th}$: *1*
Payoff: $(u_{pp}^{p,e}, u_{pp}^{p,o}), (u_{py}^{p,e}, u_{py}^{p,o})$	*(-100, -100), (-2, -2),*
$(u_{pp}^{a,e}, u_{pp}^{a,o}), (u_{py}^{a,e}, u_{py}^{a,o})$	*(2, -10), (2, -2),*
$(u_{yp}^{p,e}, u_{yp}^{p,o}), (u_{yy}^{p,e}, u_{yy}^{p,o})$	*(-2,2), (-2, -2),*
$(u_{yp}^{a,e}, u_{yp}^{a,o}), (u_{yy}^{a,e}, u_{yy}^{a,o})$	*(-2, -10), (-2, -2),*

is continuous over time, the vehicle model defined in Equation (2) can be reformed as:

$$\begin{aligned} \dot{s}_e^t &= f_e(t, s_e^t, c_e^t) \\ s_e &= [x_e, y_e, \varphi_e, v_e,]^T \\ c_e &= [\kappa_e, \alpha_e]^T \end{aligned} \tag{23}$$

where s_e is ego vehicle's state, c_e is control inputs, the function $f(\cdot)$ is piecewise continuous with respect to time t and satisfies the Lipschitz condition. We suppose that the other agents also have similar kinematics model of equation (23).

To achieve safe interaction and collision avoidance between agents, it is necessary to avoid scenarios in which multiple agents entering a certain region at the same moment, such as intersections and merging areas of adjacent roads. These regions can be described by state-value functions of agents.

1) FIELD OF REACHABILITY (FOR)

Refers to the set of possible states that can be reached by the dynamic agent i at $t \geq t_0$, given the state $s_i^{t_0} \in s_i$ of the initial t_0 and the control input $c_i^{t_0} \in c_i$. The FOR of the agent i is:

$$\begin{aligned} FOR_i(t, c_i) := \{s_i^t \in s_i | \exists s_i^{t_0} \in s_i, \exists c_i^{t_0} \in c_i, \\ \forall t \geq t_0, \dot{s}_i^t = f_i(t, s_i^t, c_i^t)\} \end{aligned} \tag{24}$$

2) FIELD OF DANGER (FOD)

The field of danger refers to the set of possible states that the autonomous agent e and other agents o can simultaneously reach a certain spatial position within a limited time period t^n under their respective initial control input $c_i^{t_0} \in c_i$. The FOD_e of e is:

$$\begin{aligned} FOD_e(t, c_e) := \{s_e^t \in FOR_e | \exists t \in [t_0, t_0 + t^n], \exists c_e^{t_0} \in c_e, \\ \exists o_i \in o, s_{o_i}^t \in FOR_{o_i}, \dot{s}_e^t = f_e(t, s_e^t, c_e), \\ ||P_e(s_e^t) - P_{o_i}(s_{o_i}^t)|| \leq d\} \end{aligned} \tag{25}$$

where $P_k(s_k^t)$ is represents the position of the agent k at time t. Whether e interacts with o can be determined based on the position subsets in their states, other subsets of states, such as speed and heading angle can be ignored if the collision occurs at the same position.

During the AV driving process, on-board sensor perception data of the surrounding environment are continuously updated with a certain frequency $1/\Delta t$. If it is found that there are visible obstacles ahead or that ''virtual'' traffic participants may randomly appear in the occluded area, the AV should adopt the best strategy in combination with the current state of motion to avoid collision accidents. Therefore, the safe driving of the ego vehicle can be described as follows:

$$SAF_e(t, c_e) := FOR_e(t, c_e) - FOD_e(t, c_e) \tag{26}$$

B. SCENARIO 1: PEDESTRIAN CROSSING (VEHICLE-HUMAN INTERACTION)

In the first experiment, as shown in Fig. 6 and Fig. 7, on a 60 m one-way two-lane road with a speed limit of 10 m/s, the AV entered the road at an initial speed of 10 m/s and approaches a crosswalk. Two large vehicles (obstacles) parked in front of the crosswalk and create occluded areas A1 and A2 for the AV. According to the traffic rules, it is illegal for pedestrians to cross the road in A1, and we set $\chi_{A1} = 0.15$. In A2, a pedestrian crossing the road is normal behavior, and we set $\chi_{A2} = 1$. The method in [2] is used to predict the potential risk probabilities of A1 and A2, $\lambda_{c,A1} = 0.12 < \lambda_{th,A1} = 0.21$ and $\lambda_{c,A2} = 0.32 > \lambda_{th,A2} = 0.04$, respectively. According to Formula (21), if a traffic participant emerges suddenly, the maximum deceleration of the AV when passing through A1 is $\alpha_{\min} = -7\ m/s^2$ ($\mu = 1$), and when passing through A2, the maximum speed change is $\alpha_{\min} = -3.5\ m/s^2$ ($\mu = 0.5$). The sensor data collection cycle step size is 0.1 second. In this case, the trajectory in each step needs to be replanned to improve the planning efficiency. After finding the occluded area, the AV initiates the proposed method. With the current input control signal, the field of reachability FOR_e and field of danger FOD_e of the AV with occluded traffic participants at the boundary of the occluded area are predicted. According to Formula (26), the field of safe driving is obtained for motion planning.

Fig. 6 shows the movement of the AV when no pedestrians emerge suddenly from A1 or A2. The bottom of Fig. 6 shows the speed profile (blue profile), acceleration profile (purple profile) and curvature profile (green profile) of the entire driving process of the AV. Since the acquisition points are discrete, three profiles are processed by cubic spline interpolation.

As can be seen in Fig. 6, the proposed method enables the AV to smoothly avoid obstacles in front of the road. The AV adopts different strategies when passing through occluded areas A1 and A2: (1) Due to the relatively low probability

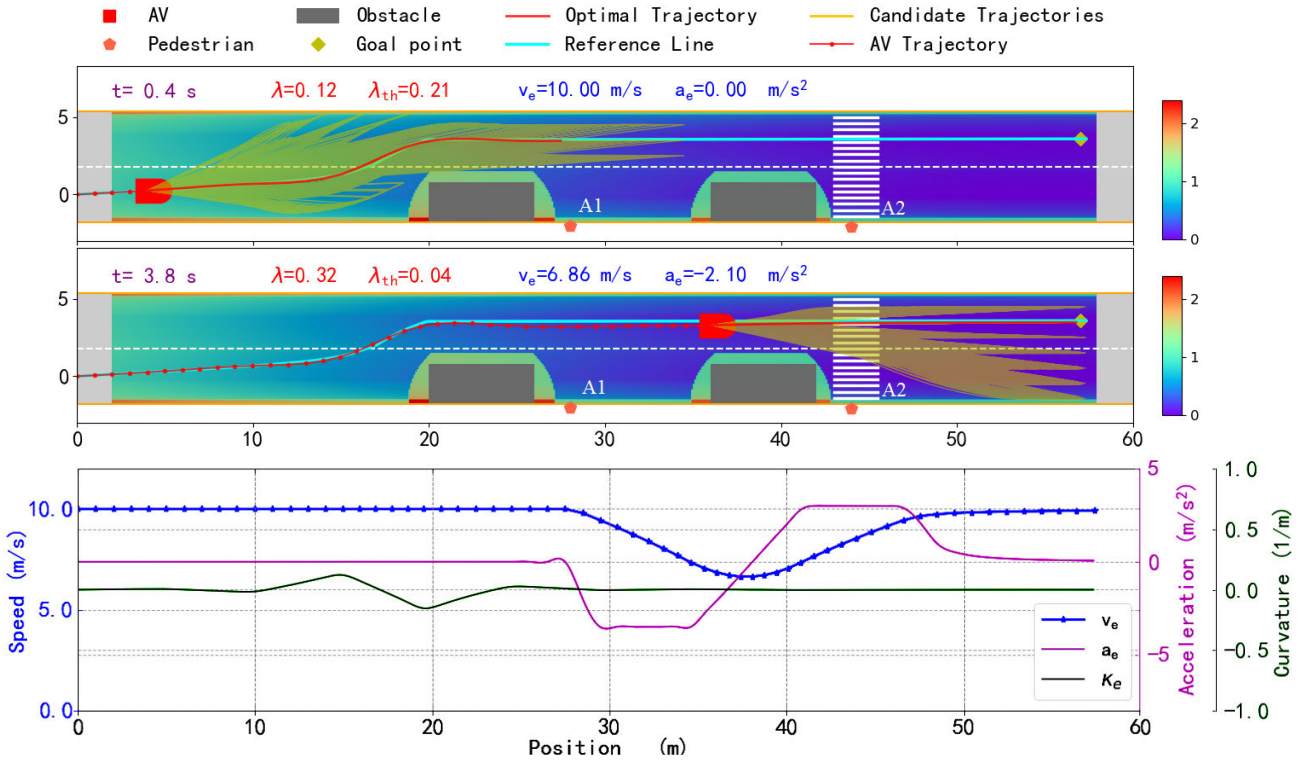

FIGURE 6. AV adopts different strategies when passing through occluded areas A1 and A2.

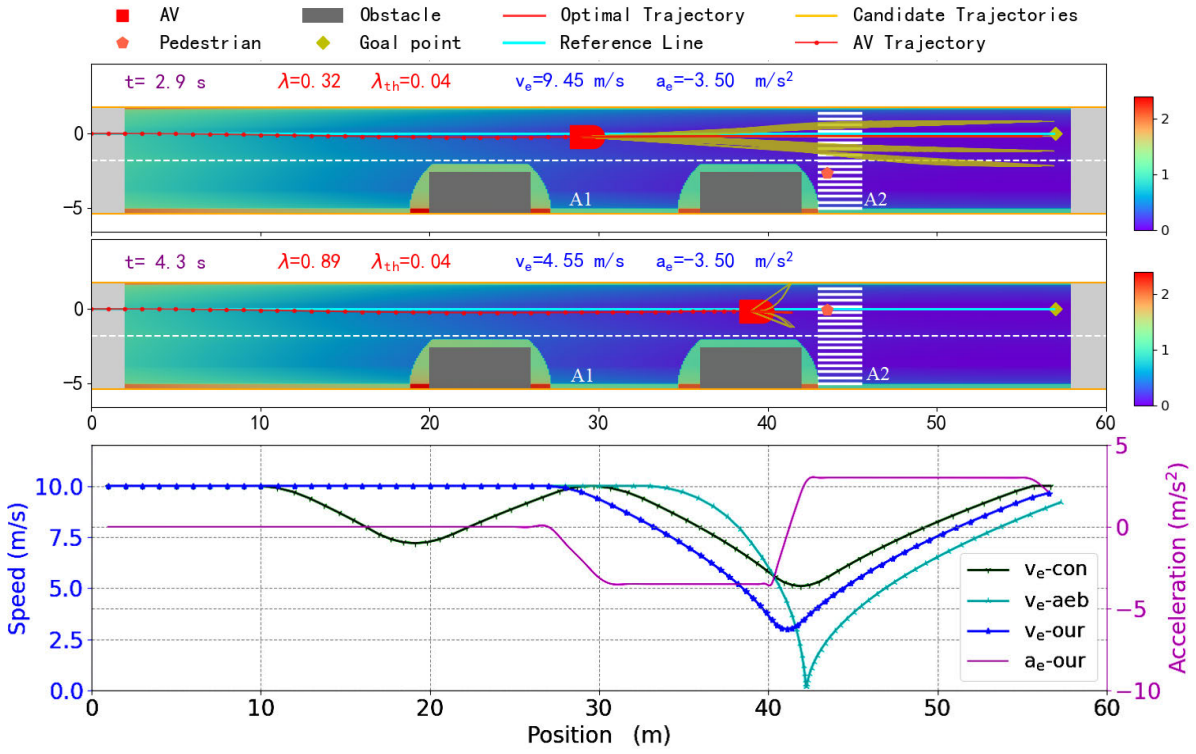

FIGURE 7. Comparison between AV using the proposed method and two existing methods after a pedestrian emerges suddenly from the occluded area A2.

of potential risk at A1, the AV uses a large deceleration to activate emergency braking if an occluded agent unexpectedly emerges from the occluded area, that is, the maximum speed change is $\dot{v}_e = \alpha_e = -7m/s^2$ ($\mu = 0.5$). Without the sudden appearance of pedestrians, the AV can pass through the occluded area A1 as quickly as possible. The speed and

TABLE 2. ($T_{aver,i}$, $DS_{aver,i}$) value obtained by Monte Carlo simulation 30,000 times.

Method	A1:10%, A2:30%	A1:10%, A2:60%	A1:10%, A2:90%
con	6.8, 1.05	7.1, 1.14	7.2, 1.22
aeb	**6.3, 0.79**	**6.5**, 1.37	**6.7**, 1.96
ours	6.7, 0.84	6.9, **0.93**	7.1, **1.02**

acceleration profiles of the AV in Fig. 6 show that when no pedestrians emerge suddenly, the AV passes through A1 at the desired speed without deceleration, which reflects the high efficiency and low conservatism of the AV; (2) A2 is a pedestrian crossing area, and its potential risk probability exceeds the threshold, which indicates a relatively high probability of pedestrians emerging suddenly. For safety and comfort, the AV uses low deceleration $\dot{v}_e = \alpha = -3.5\ m/s^2$ ($\mu = 0.5$) to pass through the occluded area A2, as shown in Fig. 6. Even if there is no sudden traffic participant at A2, the vehicle will still reduce its speed about 14 meters in front of the A2 to cross the A2 safely and comfortably.

For comparison, two existing methods were tested in this scenario. One method assumes that the collision risk in the occluded areas is always the worst-case, which is denoted by ''conservative'', for brevity, it is abbreviated as ''con''. Another approach relies on the AEB system to prevent collisions [39], which is denoted by ''aeb''. As shown in Fig. 7, at about 2.9 s, a pedestrian emerges suddenly from the occluded area A2 and was crossing the road. The purple and blue profiles are the acceleration profile and the speed profile generated by the AV using the proposed method, respectively. The green and cyan profiles are the speed profiles generated by the AV using the ''con'' method and the ''aeb'' method, respectively. By comparison, it can be seen, using the ''con'' method, the AV will always slow down through the occluded area, regardless of whether pedestrians emerge suddenly. Simply put, its behavior is relatively conservative. Using the ''aeb'' method, the AV maintains the original speed when no pedestrian emerges suddenly from the occluded area. However, the sudden appearance of traffic participants in areas with higher risk probability will cause the AV to frequently initiate emergency braking, which cannot guarantee comfort. Based on the proposed motion planning method, the AV can pass through the two occluded areas well. More specifically, the AV will move forward confidently when approaching an area with lower risk probability and activate the AEB when a pedestrian emerges suddenly, while the AV will decelerate at a comfortable rate in advance when approaching areas with higher risk probability. In contrast, the motion planning method is more comfortable than the ''aeb'' method and less conservative than the ''conservative'' method.

Considering a situation where it is difficult to justify the review results, the Monte Carlo simulation method [45] is adopted, with results that are close to the real results. The presence of traffic participants in the occluded areas of A1 and A2 is stochastic. Specifically, a 10% probability is assigned to pedestrians randomly emerging from A1, while pedestrians emerge randomly from A2 with probabilities of 30%, 60%, and 90%. Three sets of combinations of A1 and A2 are simulated, 30,000 times per set (after 30,000 simulations, the results stabilize). Each simulation calculates the time T_i and discomfort score DS_i ($i \in \{con, aeb, ours\}$) of the AV passing through the 57-meter road section in the above scenario using the three methods. Finally, the average time $T_{aver,i}$ and the average discomfort score $DS_{aver,i}$ for the 30,000 simulations are obtained. The discomfort score adopts the calculation method proposed in reference [18]:

$$DS = \frac{1}{T}\int_0^T \max(0, |a_e^t| - a_{th})dt \tag{27}$$

where a_{th} is the comfortable acceleration threshold. This paper takes $a_{th} = 3\ \mathrm{m/s^2}$. The $T_{aver,i}$ and $DS_{aver,i}$ results for each group are shown in Table 2.

From the analysis of the data in Table 2, the ''con'' method performs poorly, especially in terms of conservatism. In addition, this method has relatively poor comfort when the probability of pedestrians emerging suddenly is low because it is necessary to slow down regardless of whether the pedestrian appears. The ''aeb'' method performs relatively well when the probability of pedestrians appearing is low, since the AV decelerates less often when passing through an occluded area. With the increase in the probability of pedestrians appearing in A2, frequent activation of the AEB leads to a decrease in comfort. As indicated in Table 2, the ''aeb'' method experiences a decrease of 32%∼48% in comfort level compared to our approach when the probability of pedestrian presence within area A2 falls between 60% and 90%. The implementation of the proposed approach in AVs can overcome the limitations of the ''aeb'' method. Although autonomous vehicles still demonstrate a certain level of caution, we believe it is reasonable to exercise appropriate prudence when potential risks are high and complete situational awareness cannot be achieved.

C. SCENARIO 2: OVERTAKING (VEHICLE-VEHICLE INTERACTION)

As shown in Fig. 8, the overtaking example is built on a long, undivided, bidirectional single lane. The AV travels behind a bulky vehicle with a speed of 30 km/h at an initial speed of 32 km/h. The speed limit for both directions of traffic on the road is 40 km/h, the road centerline is assumed to be the vehicle reference line for each lane. The method in [2] is used to predict the probability of an oncoming vehicle in the oncoming traffic, the on-coming vehicle initially occluded by a vehicle ahead. At the beginning, the AV will expand the field of view through lateral movement and observe whether there is an oncoming vehicle on the oncoming traffic, then increase speed to prepare for overtaking. After changing lanes, the vehicle travels constantly at the desired speed, i.e., the road speed limit, to completes overtaking, and then returns to the original lane. During the entire overtaking process, the AV continues to observe the driving lane ahead.

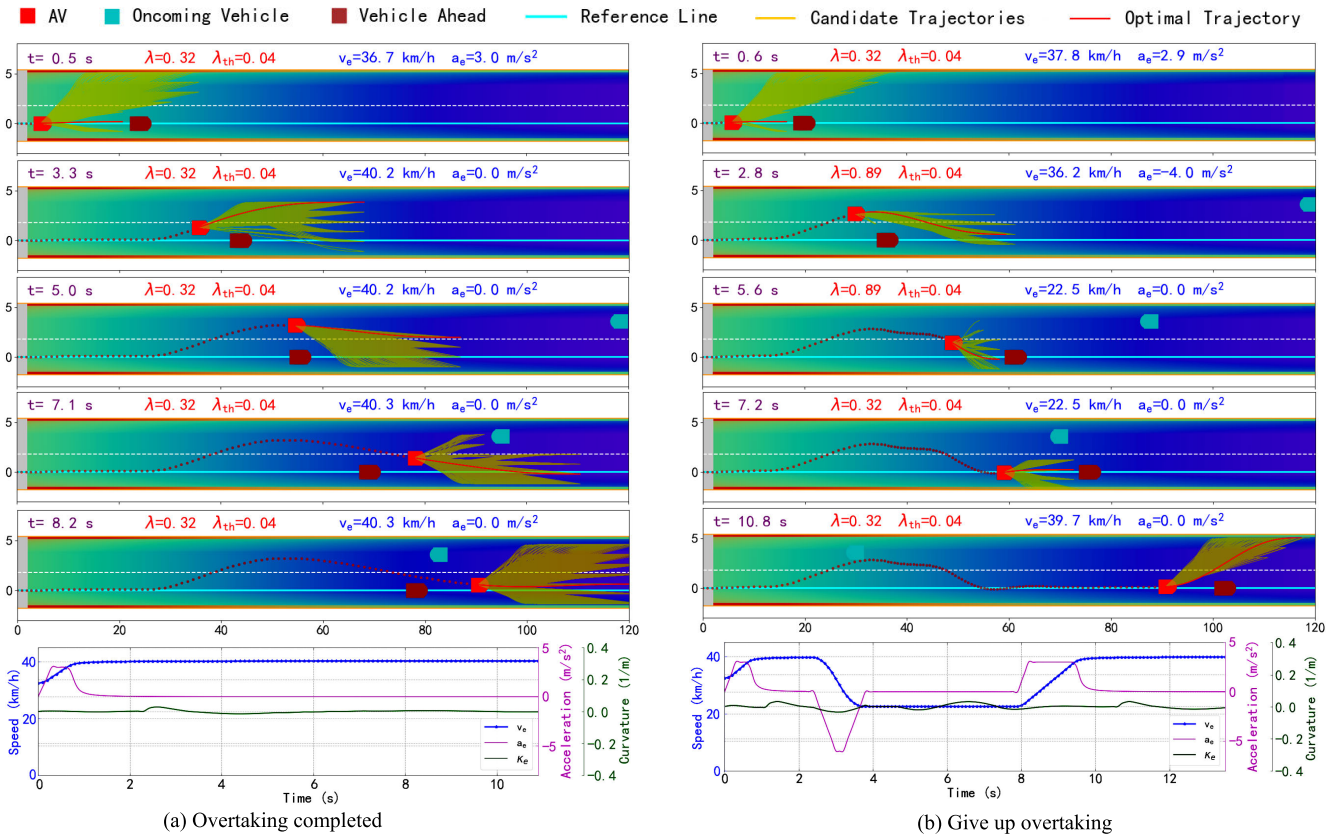

(a) Overtaking completed

(b) Give up overtaking

FIGURE 8. Overtaking simulation experiment. (a) The AV safely overtakes the bulky vehicle, merges back to the driving lane, and avoids collisions with oncoming vehicle; (b) The AV attempts to overtake the truck and safely aborted the overtaking after detecting the oncoming vehicle.

As shown in Fig. 8(a), if the vehicle's safe driving condition SAF_e is satisfied, the AV still successfully completes overtaking even if other oncoming agents enter the field of view, since it never enters the field of danger FOD_e. As shown in Fig. 8(b), if the AV determines that it will enter the field of danger FOD_e with the oncoming vehicle, the AV decelerates in time and returns to the safe state area behind the vehicle ahead. The bottom of Fig. 8 shows the corresponding speed profile (blue profile), acceleration profile (purple profile) and curvature profile (green profile) of the overtaking motion of the AV using the proposed method. Three profiles are processed by cubic spline interpolation on the sampling points.

D. SCENARIO 3: INTERSECTION (VEHICLE-VEHICLE INTERACTION)

To further verify the effectiveness of the proposed method, the AV is tested on an unprotected left turn task at an intersection without a signal light. For comparison with similar work, the scenario is recreated for validation, with the maps in [18] and set values of initial speed (9 m/s), expected speed (9 m/s), maximum acceleration (2 m/s2) and minimum acceleration (−4 m/s2). The occlusions in this scene are buildings 2 meters away from the roadside and large vehicles driving on the road, and the AV starting position is approximately 15 m away from the intersection, as shown in Fig. 9. The upper layer of Fig. 9(a) depicts the first case: the AV is driving alone at the intersection, and no other vehicles appear in the scene. The bottom layer of Fig. 9(a) depicts the second situation: a car is approaching from the left.

Fig. 9(b) and Fig. 9(c) show the speed profile and acceleration profile of the AV using the method in [18] and the proposed method, respectively. The AV in both methods can pass the intersection safely and smoothly without collisions, and the vehicle speed and heading angle do not change violently, providing good ride comfort. When no other vehicles enter the intersection, the roadside buildings block any approaching vehicles from the right. Using our proposed method, the AV is still able to smoothly pass through the intersection without deceleration with a speed of 9 m/s. According to the experiment in Scenario 1, the AV will have appropriate deceleration when moving straight through the intersection. As shown in Fig. 9(c), the proposed method enables the AV to smoothly decelerate according to the selected deceleration when another vehicle on the left enters and threatens to collide with it, thereby achieving safe driving.

To verify that the proposed method is suitable for multiple-visual-occlusion scenarios, two occluded vehicles from different directions are added to the scene in Fig. 10. The road to the right of the intersection is obscured by buildings, creating a risk of uncertainty. Through the simulation verification of the first case (scenario 3), when the initial speed is 9 m/s, without the sudden appearance of other vehicles, the AV can

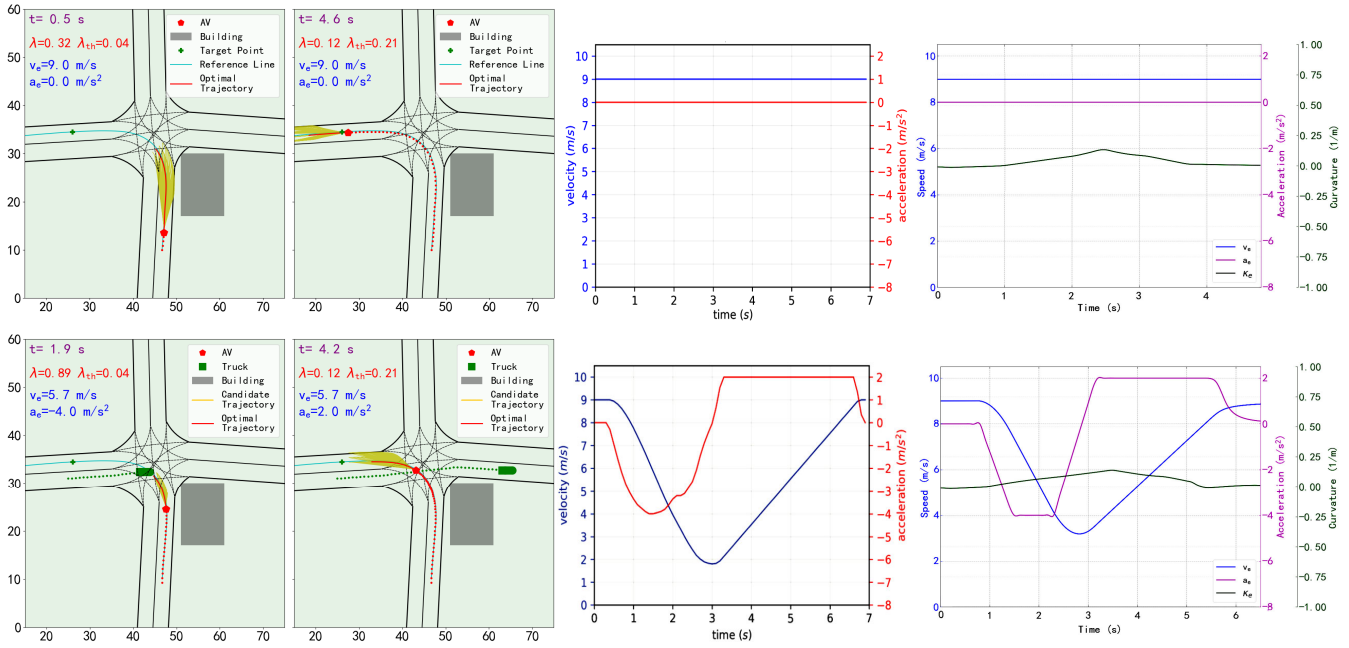

(a) Two scenarios of intersection (b) Profiles obtained by [18] (c) Profiles of ours

FIGURE 9. **(a) The first scenario (top row) is in a map with one static obstacle (building) and no incoming traffic, and the second scenario (bottom row) is in the same map with one other vehicle (green truck) coming from the left; (b) Speed and acceleration profiles obtained by [18] in two scenarios; (c) Speed, acceleration and curvature profiles obtained by proposed method in two scenarios.**

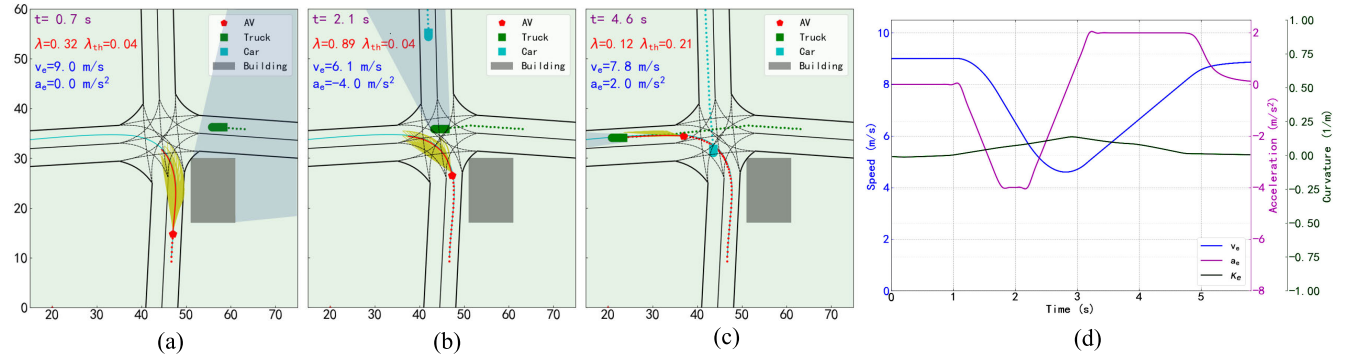

(a) (b) (c) (d)

FIGURE 10. **(a) Vehicles coming from the right road are blocked by the building; (b) Vehicles entering the intersection cause dynamic occlusion to AV; (c) AV completed the safe left turn task; (d) Profiles of the speed, acceleration and curvature of the AV turning left with time.**

pass through the intersection at a constant speed and complete the left turn requirement. In the case of a vehicle emerging suddenly from the area blocked by the building, the AV will adjust the speed according to the safe driving model FOS_e with other vehicles to avoid collision. As shown in Fig. 10, the AV starts to decelerate at 1.1 s.

When a vehicle on the right side of the road passes through the intersection, it will dynamically occlude the oncoming traffic on the road in the opposite traffic direction in front of the AV. Despite the short occlusion time, the AV cautiously continues to decelerate until the occlusion disappears. The AV gives up the right of way when oncoming traffic is approaching. When the oncoming vehicle is far away, the AV does not behave conservatively (by waiting for the oncoming vehicle to pass) but accelerates to pass through the intersection in time. As shown in Fig. 10(c), the AV completed the left turn task at 4.5 s. Fig. 10(d) shows the corresponding speed profile (blue profile), acceleration profile (red profile) and curvature profile (green profile) of the overtaking motion of the AV using the proposed method. It can be seen from the figure that the AV can turn left smoothly and effectively.

It is worth noting that there are slight changes in the curvature profile between Fig. 9 and Fig. 10, and even in Fig. 8, there are small fluctuations. This suggests that the AV encounters diverse dynamic obstacles in various scenarios, and accordingly generates real-time trajectory planning to avoid these obstacles while maintaining a comfortable ride. Therefore, further research is required to integrate safety and comfort into vehicle motion planning.

V. CONCLUSION

Autonomous driving motion planning method that considers visual occlusion environment is proposed in this paper. The results of our previously proposed method for potential risk assessment of occluded areas [2] are applied to the autonomous driving decision task. To ensure the safety, comfort, and optimal efficiency of autonomous vehicles (AVs), motion planning is approached from two perspectives: speed and heading angle. This is achieved by utilizing acceleration and curvature as control inputs. The implementation of the ''virtual game'' approach can mitigate conservatism in AVs during traffic scenarios with occlusion, thereby enhancing driving efficiency. By means of local path planning and trajectory planning in S-L coordinates, the vehicle can smoothly circumvent obstacles and achieve lateral motion. The proposed method can comprehensively consider conservatism and comfort while ensuring the safety of AVs. Based on experimental results, the proposed method is suitable for autonomous driving motion planning in urban environments with visual occlusion.

Motion planning can mitigate various negative effects that impede the development of autonomous driving technology, such as safety hazards, conservatism, and discomfort. Building upon the current work, future efforts will focus on integrating and collaboratively planning other vehicle information, as well as processing heterogeneous traffic scenarios involving various vehicles and pedestrians. This will further mitigate the impact of limited perception on motion planning. Additionally, it is imperative to deploy this method onto a hardware platform for real-world driving testing.

REFERENCES

[1] S. Gilroy, E. Jones, and M. Glavin, ''Overcoming occlusion in the automotive environment—A review,'' *IEEE Trans. Intell. Transp. Syst.*, vol. 22, no. 1, pp. 23–35, Jan. 2021.

[2] D. Wang, W. Fu, Q. Song, and J. Zhou, ''Potential risk assessment for safe driving of autonomous vehicles under occluded vision,'' *Sci. Rep.*, vol. 12, no. 1, p. 4981, Mar. 2022.

[3] Y. Yoshihara, Y. Morales, N. Akai, E. Takeuchi, and Y. Ninomiya, ''Autonomous predictive driving for blind intersections,'' in *Proc. IEEE/RSJ Int. Conf. Intell. Robots Syst. (IROS)*, Sep. 2017, pp. 3452–3459.

[4] P. F. Orzechowski, A. Meyer, and M. Lauer, ''Tackling occlusions & limited sensor range with set-based safety verification,'' in *Proc. 21st Int. Conf. Intell. Transp. Syst. (ITSC)*, Nov. 2018, pp. 1729–1736.

[5] Ö. Ş. Taş and C. Stiller, ''Limited visibility and uncertainty aware motion planning for automated driving,'' in *Proc. IEEE Intell. Vehicles Symp. (IV)*, Jun. 2018, pp. 1171–1178.

[6] M. Naumann, H. Konigshof, M. Lauer, and C. Stiller, ''Safe but not overcautious motion planning under occlusions and limited sensor range,'' in *Proc. IEEE Intell. Vehicles Symp. (IV)*, Jun. 2019, pp. 140–145.

[7] P. Narksri, H. Darweesh, E. Takeuchi, Y. Ninomiya, and K. Takeda, ''Occlusion-aware motion planning with visibility maximization via active lateral position adjustment,'' *IEEE Access*, vol. 10, pp. 57759–57782, 2022.

[8] E. Debada, A. Ung, and D. Gillet, ''Occlusion-aware motion planning at roundabouts,'' *IEEE Trans. Intell. Vehicles*, vol. 6, no. 2, pp. 276–287, Jun. 2021.

[9] X. Ren, T. Yang, L. E. Li, A. Alahi, and Q. Chen, ''Safety-aware motion prediction with unseen vehicles for autonomous driving,'' in *Proc. IEEE/CVF Int. Conf. Comput. Vis. (ICCV)*, Oct. 2021, pp. 15711–15720.

[10] Y. Nager, A. Censi, and E. Frazzoli, ''What lies in the shadows? Safe and computation-aware motion planning for autonomous vehicles using intent-aware dynamic shadow regions,'' in *Proc. Int. Conf. Robot. Autom. (ICRA)*, May 2019, pp. 5800–5806.

[11] J. Müller, J. Strohbeck, M. Herrmann, and M. Buchholz, ''Motion planning for connected automated vehicles at occluded intersections with infrastructure sensors,'' *IEEE Trans. Intell. Transp. Syst.*, vol. 23, no. 10, pp. 17479–17490, Oct. 2022.

[12] V. Narri, A. Alanwar, J. Mårtensson, C. Norén, L. D. Col, and K. H. Johansson, ''Set-membership estimation in shared situational awareness for automated vehicles in occluded scenarios,'' in *Proc. IEEE Intell. Vehicles Symp. (IV)*, Jul. 2021, pp. 385–392.

[13] C. Katrakazas, M. Quddus, and W.-H. Chen, ''A new integrated collision risk assessment methodology for autonomous vehicles,'' *Accident Anal. Prevention*, vol. 127, pp. 61–79, Jun. 2019.

[14] F. Damerow, T. Puphal, Y. Li, and J. Eggert, ''Risk-based driver assistance for approaching intersections of limited visibility,'' in *Proc. IEEE Int. Conf. Veh. Electron. Saf. (ICVES)*, Jun. 2017, pp. 178–184.

[15] R. Poncelet, A. Verroust-Blondet, and F. Nashashibi, ''Safe geometric speed planning approach for autonomous driving through occluded intersections,'' in *Proc. 16th Int. Conf. Control, Autom., Robot. Vis. (ICARCV)*, Dec. 2020, pp. 393–399.

[16] M. Lee, M. Sunwoo, and K. Jo, ''Collision risk assessment of occluded vehicle based on the motion predictions using the precise road map,'' *Robot. Auto. Syst.*, vol. 106, pp. 179–191, Aug. 2018.

[17] M.-Y. Yu, R. Vasudevan, and M. Johnson-Roberson, ''Risk assessment and planning with bidirectional reachability for autonomous driving,'' in *Proc. IEEE Int. Conf. Robot. Autom. (ICRA)*, Aug. 2020, pp. 5363–5369.

[18] M.-Y. Yu, R. Vasudevan, and M. Johnson-Roberson, ''Occlusion-aware risk assessment for autonomous driving in urban environments,'' *IEEE Robot. Autom. Lett.*, vol. 4, no. 2, pp. 2235–2241, Apr. 2019.

[19] L. Y. Morales, A. Naoki, Y. Yoshihara, and H. Murase, ''Towards predictive driving through blind intersections,'' in *Proc. 21st Int. Conf. Intell. Transp. Syst. (ITSC)*, Nov. 2018, pp. 716–722.

[20] C. Zhang, F. Steinhauser, G. Hinz, and A. Knoll, ''Improved occlusion scenario coverage with a POMDP-based behavior planner for autonomous urban driving,'' in *Proc. IEEE Int. Intell. Transp. Syst. Conf. (ITSC)*, Sep. 2021, pp. 593–600.

[21] C. Hubmann, N. Quetschlich, J. Schulz, J. Bernhard, D. Althoff, and C. Stiller, ''A POMDP maneuver planner for occlusions in urban scenarios,'' in *Proc. IEEE Intell. Vehicles Symp. (IV)*, Jun. 2019, pp. 2172–2179.

[22] P. Narksri, E. Takeuchi, Y. Ninomiya, and K. Takeda, ''Crossing blind intersections from a full stop using estimated visibility of approaching vehicles,'' in *Proc. IEEE Intell. Transp. Syst. Conf. (ITSC)*, Oct. 2019, pp. 2427–2434.

[23] M. Schratter, M. Bouton, M. J. Kochenderfer, and D. Watzenig, ''Pedestrian collision avoidance system for scenarios with occlusions,'' in *Proc. IEEE Intell. Vehicles Symp. (IV)*, Jun. 2019, pp. 1054–1060.

[24] S. Thornton, ''Autonomous vehicle speed control for safe navigation of occluded pedestrian crosswalk,'' 2018, *arXiv:1802.06314*.

[25] Z. Qiao, K. Muelling, J. Dolan, P. Palanisamy, and P. Mudalige, ''POMDP and hierarchical options MDP with continuous actions for autonomous driving at intersections,'' in *Proc. 21st Int. Conf. Intell. Transp. Syst. (ITSC)*, Nov. 2018, pp. 2377–2382.

[26] D. Isele, R. Rahimi, A. Cosgun, K. Subramanian, and K. Fujimura, ''Navigating occluded intersections with autonomous vehicles using deep reinforcement learning,'' in *Proc. IEEE Int. Conf. Robot. Autom. (ICRA)*, May 2018, pp. 2034–2039.

[27] M. Bouton, A. Nakhaei, K. Fujimura, and M. J. Kochenderfer, ''Safe reinforcement learning with scene decomposition for navigating complex urban environments,'' in *Proc. IEEE Intell. Vehicles Symp. (IV)*, Jun. 2019, pp. 1469–1476.

[28] D. Kamran, C. Fernandez Lopez, M. Lauer, and C. Stiller, ''Risk-aware high-level decisions for automated driving at occluded intersections with reinforcement learning,'' in *Proc. IEEE Intell. Vehicles Symp. (IV)*, Nov. 2020, pp. 1205–1212.

[29] M. Althoff and S. Magdici, ''Set-based prediction of traffic participants on arbitrary road networks,'' *IEEE Trans. Intell. Vehicles*, vol. 1, no. 2, pp. 187–202, Jun. 2016.

[30] K. Sama, Y. Morales, H. Liu, N. Akai, A. Carballo, E. Takeuchi, and K. Takeda, ''Extracting human-like driving behaviors from expert driver data using deep learning,'' *IEEE Trans. Veh. Technol.*, vol. 69, no. 9, pp. 9315–9329, Sep. 2020.

[31] Y. Akagi and P. Raksincharoensak, "Stochastic driver speed control behavior modeling in urban intersections using risk potential-based motion planning framework," in *Proc. IEEE Intell. Vehicles Symp. (IV)*, Jul. 2015, pp. 368–373.
[32] L. Wang, C. Fetnandez Lopez, and C. Stiller, "Generating efficient behaviour with predictive visibility risk for scenarios with occlusions," in *Proc. IEEE 23rd Int. Conf. Intell. Transp. Syst. (ITSC)*, Sep. 2020, pp. 1–7.
[33] H. Andersen, J. Alonso-Mora, Y. H. Eng, D. Rus, and M. H. Ang, "Trajectory optimization and situational analysis framework for autonomous overtaking with visibility maximization," *IEEE Trans. Intell. Vehicles*, vol. 5, no. 1, pp. 7–20, Mar. 2020.
[34] M. Koç, E. Yurtsever, K. Redmill, and Ü. Özgüner, "Pedestrian emergence estimation and occlusion-aware risk assessment for urban autonomous driving," in *Proc. IEEE Int. Intell. Transp. Syst. Conf. (ITSC)*, Sep. 2021, pp. 292–297.
[35] Z. Zhang and J. F. Fisac, "Safe occlusion-aware autonomous driving via game-theoretic active perception," 2021, *arXiv:2105.08169*.
[36] E. Bicho, P. Mallet, and G. Schoner, "Using attractor dynamics to control autonomous vehicle motion," in *Proc. 24th Annu. Conf. IEEE Ind. Electron. Soc. (IECON)*, Aug. 1998, pp. 1176–1181.
[37] C. Zhang, D. Chu, S. Liu, Z. Deng, C. Wu, and X. Su, "Trajectory planning and tracking for autonomous vehicle based on state lattice and model predictive control," *IEEE Intell. Transp. Syst. Mag.*, vol. 11, no. 2, pp. 29–40, 2019.
[38] X. Lin, J. Zhang, J. Shang, Y. Wang, H. Yu, and X. Zhang, "Decision making through occluded intersections for autonomous driving," in *Proc. IEEE Intell. Transp. Syst. Conf. (ITSC)*, Oct. 2019, pp. 2449–2455.
[39] T. Shimizu and P. Raksincharoensak, "Motion planning via optimization of risk quantified by collision velocity accompanied with AEB activation," in *Proc. IEEE Int. Conf. Veh. Electron. Saf. (ICVES)*, Jun. 2017, pp. 19–25.
[40] L. Sun, W. Zhan, M. Tomizuka, and A. D. Dragan, "Courteous autonomous cars," in *Proc. IEEE/RSJ Int. Conf. Intell. Robots Syst. (IROS)*, Oct. 2018, pp. 663–670.
[41] F. Camara, P. Dickinson, and C. Fox, "Evaluating pedestrian interaction preferences with a game theoretic autonomous vehicle in virtual reality," *Transp. Res. F, Traffic Psychol. Behaviour*, vol. 78, pp. 410–423, Apr. 2021.
[42] H. Hu and H. W. Stuart Jr., "An epistemic analysis of the Harsanyi transformation," *Int. J. Game Theory*, vol. 30, no. 4, pp. 517–525, May 2002.
[43] S. Çinar, Ş. Yilmaz, and B. Öz, "Pedestrians' crossing behaviors and crossing preferences: A field study," *Trans. Transp. Sci.*, vol. 13, no. 2, pp. 18–26, Aug. 2022.
[44] L. I. Juan-Liu, *Research on Pedestrian Crossing Behavior at Mid-Block Street Crosswalk*. Changsha, China: Changsha Univ. Science Technology, 2014.
[45] J. M. Hammersley and D. C. Handscomb, *Solution of Linear Operator Equations* (Monte Carlo Methods). New York, NY, USA: Methuen & Co, 1964, ch. 7, pp. 85–96.

DENGGUI WANG received the B.S. and M.S. degrees in electrical engineering from Northwest A&F University, Xi'an, China, in 2004 and 2007, respectively. He is currently pursuing the Ph.D. degree in mechanical engineering with the School of Mechanical and Precision Instrument Engineering, Xi'an University of Technology, Xi'an. His research interest includes automated driving. His current research interests include potential risk assessment and motion planning of autonomous vehicle.

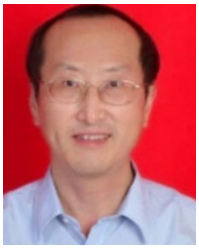

WEIPING FU received the Ph.D. degree in mechanical design and theory from Xi'an Jiaotong University, Xi'an, China, in 1996. He is currently a Professor with the College of Mechanical and Precision Instrument Engineering, Xi'an University of Technology. His research interests include intelligent robot, modern logistics system engineering and technology, intelligent vehicle and its control theory and technology, electromechanical systems, and manufacturing system dynamics and control.

JINCAO ZHOU received the M.Sc. and Ph.D. degrees in vehicle engineering from Chang'an University, Xi'an, China, in 2014 and 2018, respectively. He is currently a Lecturer with the College of Mechanical and Precision Instrument Engineering, Xi'an University of Technology. His research interests include vehicle active safety and computer vision.

QINGYUAN SONG received the M.Sc. degree in power engineering from the Lanzhou University of Technology, in 2014. He is currently pursuing the Ph.D. degree in mechanical engineering with the School of Mechanical and Precision Instrument Engineering, Xi'an University of Technology. His current research interests include cognition and decision-making technology of autonomous vehicle.